

Analytical and Numerical Investigation of Free Vibration in Beams under Diverse Boundary Conditions and Material Characteristics

Kipkirui Chepkwony

PG Student, Department of Mechanical Engineering, Andhra University, Visakhapatnam

Ch. Ratnam

Professor, Department of Mechanical Engineering, Andhra University, Visakhapatnam

Abstract: Beams are defined by considering their boundary conditions. This paper focused on the Free Vibration Analysis of SiC aluminium-reinforced composite beams by considering four boundary conditions i.e. clamped-free, clamped-clamped, clamped-simply supported, and simply supported. The study utilized the Euler-Bernoulli beam theory to obtain the frequency equation and numerical simulations on the ANSYS Workbench to analyze the free vibration behaviour. The results obtained for SiC aluminium-reinforced composite are compared with those of Aluminium and steel material. The study demonstrates that boundary conditions affect the dynamic response of the composite beams, with clamped-clamped boundary conditions yielding higher natural frequencies, followed by clamped-simply supported, simply supported, and clamped-free boundary conditions yielding low natural frequencies. Furthermore, the natural frequencies of SiC/Aluminium composite beams are higher than those of unreinforced Aluminium and steel beams. The study found that the natural frequency of vibrations increases linearly with an increase in the cross-section area of the beam. Finally, the study found that the natural frequency of vibrations increases with an increase in the specific modulus of the material.

Keywords: Natural frequency, Boundary Conditions, SiC/Aluminium composites, Free Vibration Analysis, Euler-Bernoulli Theory, Finite Element Analysis.

(A). INTRODUCTION

With the advances in technology, composite materials have become the preferred choice for constructing mechanical equipment and structures. Silicon Carbide (SiC) reinforced Aluminium composites are among the best lightweight composites used in high-performance applications. These composites are low in density but have high strength and stiffness, making them suitable for applications in the aerospace industry and lightweight structures. In that connection, the study of the vibration characteristics of composite beams is a significant and distinctive area of focus in the field of mechanical engineering. It is particularly essential to quantify the impact of dynamic loading on structures such as tall buildings, long bridges, and industrial machinery. Dynamic loading can lead to fatigue and the initiation of cracks, which are major contributors to accidents and failures in industrial machinery.

Lu et. al. [1] investigated the effect of the vibration frequency on the fatigue of strength of 6061-T6 Al Alloys through two stress analysis methods namely nominal and hot-spot stress. Mufazzal et al [2] explored the effect of material and surface cracks on the free vibration of the cantilever beam. Agarwallaa and Parhib [3] highlighted that, at the point where cracks appear, the vibration frequency is high. The study was conducted experimentally and with the help of Fine Element software.

Nikhil and Jeyashree [4] investigated the dynamic response of a cracked beam to free vibration. The study utilized ANSYS the effects of cracks at different locations and depths in cantilever beams, fixed-fixed beams, and simply supported beams. Mia et.al.[5] studied the natural frequency and mode shapes of transverse vibration on the cracked and uncracked cantilever beams. The analysis was extended to find the impact of crack opening size and mesh refinement. Gawande and More [6] performed free vibration analysis to investigate the effect of the notch on the dynamics of cantilever beams using ANSYS and experiment. The study accounted for the depth and position of the notch in the beam.

Kuppast et al [7] used ANSYS and experimental modelling to investigate the vibration properties of aluminium alloys. The study simulates the effect of increasing copper and silicon content in aluminium alloys. Abdellah et al. [8] investigate the vibration behaviour of aluminium and its alloys. The samples were designed as cantilever plates with and without holes. The analysis was performed with Ansys. Derkach et al. [9] analyzed the effect of the notch on the fundamental mode of vibration for composite cantilever beams using the Finite element analysis.

Quila et al. [10] studied the free vibration analysis of an uncracked and cracked fixed beam using ANSYS. Ferreira and Neto [11] modelled active Ni-Ti filament-reinforced hybrid adaptive composite beams under free-free boundary conditions to study vibration modes and their frequencies. Avcar [12] investigates the free vibration of square cross-sectioned Aluminium beams both analytically and numerically under four different boundary conditions. Haskul and Kisa [13] investigate the free vibration of a

double-tapered beam with linearly varying thickness and width using finite element and component mode synthesis methods. Rossit et al. [14] investigate the vibrational behaviour of L-shaped beams with cracks. The transversal displacements were described using the Euler-Bernoulli beam theory, while the crack was modelled as an elastically restrained hinge. Wang and Qiao [15] study the vibration behaviour of beams with arbitrary discontinuities and boundary conditions. Charoensuk and Sethaput [16] performed a vibration analysis experiment and finite element analysis on metal plates with V-notch at multiple notch locations. Shah et al. [17] used ANSYS to perform the free vibration of composite beams and obtained fundamental natural frequencies. Bozkurt et al. [18] explore analytical approximation techniques in transverse vibration analysis of beams. The computations were performed using the Adomian Decomposition Method (ADM), the Variational Iteration Method (VIM), and the Homotopy Perturbation Method (HPM). Nalbant et al. [19] investigated the free vibration behaviour of stepped nano-beams using the Bernoulli-Euler theory for beam analysis and Eringen's nonlocal elasticity theory for nanoscale analysis. The system's boundary conditions were defined as simply supported. Teggi [20] explores the free vibration of steel beams under two different boundary conditions: Clamped-Free (C-F) and Clamped-Clamped (C-C). Santhosh et al. [21] conducted vibration tests on Aluminium 5083 reinforced with varying percentage weights of Silicon Carbide (SiC) and fly ash through experimentation. Bozkurt and Ersoy [22] investigated the vibration behaviour of metal matrix composites (MMCs) used in the aerospace industry

using finite element analysis (FEM). The study focused on AA2124/SiC/25p, a particle-reinforced MMC with a homogeneous distribution of particles, hence commonly used in aerospace applications. Acharya et al. [23] analyzed the dynamic characteristics of Aluminium 6061 plates. Modal analysis was performed using both simulation and experimental methods. Kumar et al. [24] conducted a modal analysis of AA5083 composite material reinforced with multi-wall carbon nanotubes using analytical and Finite element methods. Taj et al. [25] studied the vibrational characteristics of Aluminium graphite metal matrix composites. The study evaluated the natural frequencies and mode shapes of the composites by experiments and finite element analysis methods. Lakshmikanthan et al. [26] performed the free vibration analysis of A357 Alloy reinforced with dual-particle size Silicon Carbide Metal Matrix composite plates using the Finite Element Method. The study examined the natural frequencies and mode shapes of the composite plates under Clamped-Clamped and Simply Supported-Simply Supported boundary conditions. In this paper, free vibration analysis on SiC/Aluminium composite beams will be performed. This study will focus on the effects of the four types of boundary conditions, namely, C-F, C-C, C-SS, and SS-SS, on the natural frequencies and mode shapes of the beams. Additionally, the effects of the mechanical properties of the SiC/Aluminium composite on the fundamental natural frequencies of vibration will also be evaluated. These results will be compared to the results of unreinforced aluminium and steel material

(B). ANALYTICAL FORMULATIONS

(i). Halpin-Tsai equation

Since SiC/Aluminium is a particulate composite, the Halpin-Tsai equation predicts the Young Modulus of Elasticity. The equation is as follows:

$$E_c = \frac{E_m((1+2sqV_p))}{1-qV_p} \quad (1)$$

$$\text{Where } q = \frac{\left(\frac{E_p}{E_m} - 1\right)}{\left(\frac{E_p}{E_m} + 2s\right)} \quad (2)$$

E_c = Composite Young Modulus, E_p = Particles Young Modulus, E_m = Matrix Young Modulus, V_p = Particles Volume, s = Particle Aspect ratio (1 – 2)

(ii). Rule of Mixtures

By application of the rule of mixtures, the density of the composite is obtained as follows:

$$\rho_c = \rho_p V_p + \rho_m V_m \quad (3)$$

ρ_c = Density of composite ρ_p = Density of SiC particles
 ρ_m = Density of Aluminium Matrix

V_p = SiC Particles Volume V_m = Aluminium Matrix Volume

(iii). Governing Equation formulations

Let's apply the Euler-Bernoulli Beam theory to a beam with length L and uniform cross-section. A is considered. Assuming the beam to be elastic with Young's Modulus E, and the Density ρ .

The relationship between the bending moment and deflection can be expressed as:

$$M = EI \frac{d^2y}{dx^2} \quad (4)$$

Where E is Young's Modulus, I is the moment of inertia of the beam and y is the deflection of the beam. For a uniform homogenous beam, the equation of motion is obtained as:

$$\frac{EI}{\rho A} \frac{d^4y}{dx^4} + \frac{d^2y}{dt^2} = 0, \text{ for } 0 \leq x \leq L \quad (5)$$

Where ρ is Density, and A is the cross-section area of the beam.

Then,

$$c^2 \frac{d^4y}{dx^4} + \frac{d^2y}{dt^2} = 0, \text{ for } 0 \leq x \leq L \quad (6)$$

$$\text{Where } c = \sqrt{\frac{EI}{\rho A}} \quad (7)$$

The solution of equation (5) is obtained by the method of separation of variables thus, one part depends on position and the other part depends on time.

$$y = W(x)T(t) \quad (8)$$

Where W is independent of time and T is independent of position. Substituting equation (8) into equation (6) and simplifying we get,

$$\frac{c^2}{W(x)} \frac{d^4 W(x)}{dx^4} = \frac{1}{T(t)} \frac{d^2 T(t)}{dt^2} \quad (9)$$

The Equation (9) is expressed as two separate differential equations:

Position variable: $\frac{d^4 W}{dx^4} - \beta^4 W(x) = 0$ (10)

Where $\beta^4 = \frac{\omega^2}{c^2} = \frac{\rho A \omega^2}{EI}$ (11)

Time variable: $\frac{d^2 T(x)}{dt^2} + \omega^2 T(t) = 0$ (12)

The general solution for equation (10) is:

$$W(x) = C_1 \sinh \beta x + C_2 \cosh \beta x + C_3 \sin \beta x + C_4 \cos \beta x \quad (13)$$

$C_1, C_2, C_3,$ and C_4 are constants, they are obtained by considering boundary conditions, and \sinh and \cosh , are the hyperbolic functions.

To solve equation (13), we consider the following conditions:

(a) Clamped-Free (C-F) beam

The boundary conditions are;

At $x = 0, w(x) = 0$ and $\frac{dw}{dx} = 0$ (14)

At $x = L, \frac{d^2 w}{dx^2} = 0$ and $\frac{d^3 w}{dx^3} = 0$ (15)

When the above boundary conditions are considered in equation (13),

$$C_1 = 0, \quad C_3 = 0$$

By simplifications, the following matrix expression is obtained.

$$\begin{bmatrix} \sinh \beta L + \sin \beta L & \cosh \beta L + \cos \beta L \\ \cosh \beta L + \cos \beta L & \sinh \beta L - \sin \beta L \end{bmatrix} \begin{bmatrix} C_2 \\ C_4 \end{bmatrix} = \begin{bmatrix} 0 \\ 0 \end{bmatrix} \quad (16)$$

For a nontrivial solution of C_2 and C_4 then obtaining the determinant of the coefficients will be zero. Then the solution is as follows:

$$\cos \beta L \cosh \beta L = -1 \quad (17)$$

The first three roots of equation (17) are determined numerically using the MATLAB commands code. The roots βL are referred to as eigenvalues.

$$\beta L = 1.87510 \text{ for } n = 1 \quad \beta L = 4.69409 \text{ for } n = 2 \quad \beta L = 7.85340 \text{ for } n = 3$$

Where n is the mode number. (18)

(b) Clamped-Clamped (C-C) beam

The boundary conditions for the C-C beam are;

At $x = 0, w(x) = 0$ and $\frac{dw}{dx} = 0$ (19)

At $x = L, w(L) = 0$ and $\frac{dw}{dx} = 0$ (20)

When the above boundary conditions are considered in equation (13),

$$C_2 = 0, \quad C_4 = 0$$

By simplifications, the following matrix expression is obtained.

$$\begin{bmatrix} \sinh \beta L - \sin \beta L & \cosh \beta L - \cos \beta L \\ \cosh \beta L - \cos \beta L & \sinh \beta L + \sin \beta L \end{bmatrix} \begin{bmatrix} C_1 \\ C_3 \end{bmatrix} = \begin{bmatrix} 0 \\ 0 \end{bmatrix} \quad (21)$$

For a nontrivial solution of C_1 and C_3 then obtaining the determinant of the coefficients will be zero. Then the solution is as follows:

$$\cos \beta L \cosh \beta L = 1 \quad (22)$$

The first three roots of equation (22) are determined numerically using the MATLAB commands code. The roots βL are referred to as eigenvalues.

$$\beta L = 4.73004 \text{ for } n = 1, \quad \beta L = 7.85321 \text{ for } n = 2, \quad \beta L = 10.9956 \text{ for } n = 3$$

Where n is the mode number. (23)

(c) Clamped-Simply Supported (C-SS) beam

The boundary conditions for the C-SS beam are;

At $x = 0, w(x) = 0$ and $\frac{dw}{dx} = 0$ (24)

At $x = L, w(L) = 0$ and $\frac{d^2 w}{dx^2} = 0$ (25)

When the above boundary conditions are considered in equation (13),

$$C_2 + C_3 = 0$$

By simplifications, the following matrix expression is obtained

$$\begin{bmatrix} \sinh \beta L - \sin \beta L & \cosh \beta L - \cos \beta L \\ \sinh \beta L + \sin \beta L & \cosh \beta L + \cos \beta L \end{bmatrix} \begin{bmatrix} C_1 \\ C_2 \end{bmatrix} = \begin{bmatrix} 0 \\ 0 \end{bmatrix} \quad (26)$$

For a nontrivial solution of C_1 and C_2 then obtaining the determinant of the coefficients will be zero. Then the solution is as follows:

$$\tanh \beta L = \tan \beta L \quad (27)$$

The first three roots of equation (27) are determined numerically using the MATLAB commands code provided in Appendix 1. The roots βL are referred to as eigenvalues.

$$\beta L = 3.9266 \text{ for } n = 1, \quad \beta L = 7.0686 \text{ for } n = 2, \quad \beta L = 10.2102 \text{ for } n = 3$$

Where n is the mode number. (28)

(d) Simply Supported-Simply Supported (SS-SS) beam

The boundary conditions for the SS-SS beam are;

At $x = 0, w(x) = 0$ and $\frac{d^2 w}{dx^2} = 0$ (29)

At $x = L, w(L) = 0$ and $\frac{d^2 w}{dx^2} = 0$ (30)

When the above boundary conditions are considered in equation (13),

$$C_1 = 0, \quad C_2 = 0$$

By simplifications, the following matrix expression is obtained

$$\begin{bmatrix} \sinh \beta L & \sin \beta L \\ \sinh \beta L & -\sin \beta L \end{bmatrix} \begin{bmatrix} C_3 \\ C_4 \end{bmatrix} = \begin{bmatrix} 0 \\ 0 \end{bmatrix} \quad (31)$$

For a nontrivial solution of C_3 and C_4 then obtaining the determinant of the coefficients will be zero. Then the solution is as follows:

$$\sin \beta L \sinh \beta L = 0 \quad (32)$$

The first three roots of equation (32) are determined numerically using the MATLAB commands code provided in Appendix 1. The roots βL are referred to as eigenvalues.

$\beta L = 3.14159$ for $n = 1$, $\beta L = 6.28318$ for $n = 2$,
 $\beta L = 9.42478$ for $n = 3$ Where n is the mode number.
 (33)

Equations 17, 22, 27, and 32 are called frequency equations. By rearranging equation 11, it can be expressed as follows:

$$\omega_n = (\beta_n L)^2 \sqrt{\frac{EI}{\rho A L^4}}, \text{ Where } n=1,2, 3, \dots n \text{ modes numbers.} \quad (34)$$

Table 1 Properties of materials

Properties	SiC Particles	Aluminium	Steel
Density (kg/m ³)	3210	2700	7850
Young Modulus x 10 ⁹ Pa	440	70	210
Particle Volume (V _p) in Percentage (%)	15	85	-
Aspect ratio of particles	1-2	-	-

(C). RESULTS AND DISCUSSION

(i). Natural frequency across the material:

SiC Particles and Aluminium material properties were adapted from Yuan et al. [27]. To obtain the Elastic Modulus (E_c) of the composite, the rule of mixtures is applied with the help of the Halpin-Tsai equation.

$$q = \frac{\left(\frac{440}{70} - 1\right)}{\left(\frac{440}{70} + 2(1.5)\right)} = 0.5692 = 96.14 \text{ Gpa}$$

$$E_c = \frac{70 \times 10^9 \left((1 + 2(1.5)(0.5692)(0.15)) \right)}{1 - ((0.5692)(0.15))}$$

$$\rho_c = \rho_p V_p + \rho_m V_m,$$

$$\rho_c = (3210 \times 0.15) + (2700 \times 0.85) = 2777 \text{ Kg/m}^3$$

Problem: To demonstrate the vibration analysis of the beam, the model with the following dimensional characteristics is considered for evaluation: Length (L) = 500mm, width (b) = 50mm, depth (d) = 10mm.

Table 2 Natural Frequency of Clamped-Free (C-F) beam

Mode	Method	SiC/Aluminium Composite	Aluminium	Steel
		Natural Frequency 'f' in Hz		
Mode 1	Analytical	38.02	32.90	33.42
	Ansys	38.45	32.91	33.65
Mode 2	Analytical	238.29	206.17	209.43
	Ansys	240.51	205.86	210.51
Mode 3	Analytical	666.98	577.08	586.20
	Ansys	672.11	575.21	588.19

Table 3 Natural Frequency of Clamped-Clamped (C-C) beam

Mode	Method	SiC/Aluminium Composite	Aluminium	Steel
		Natural Frequency 'f' in Hz		
Mode 1	Analytical	241.95	209.34	212.65
	Ansys	246.73	210.74	215.05
Mode 2	Analytical	666.94	577.05	586.17
	Ansys	678.04	579.12	590.95
Mode 3	Analytical	1307.47	1131.25	1149.13
	Ansys	1324.60	1131.30	1154.43

Table 4 Natural Frequency of Clamped-Simply Supported (C-SS) beam

Mode	Method	SiC/Aluminium Composite	Aluminium	Steel
		Natural Frequency 'f' in Hz		
Mode 1	Analytical	166.74	144.26	146.54
	Ansys	168.40	145.40	147.37
Mode 2	Analytical	540.33	467.51	474.89
	Ansys	544.72	470.78	477.71
Mode 3	Analytical	1127.36	975.42	990.83
	Ansys	1133.80	978.74	992.08

Table 5 Natural Frequency of Simply Supported-Simply Supported (SS-SS) beam

Mode	Method	SiC/Aluminium Composite	Aluminium	Steel
		Natural Frequency 'f' in Hz		
Mode 1	Analytical	109.92	92.35	93.81
	Ansys	106.71	92.33	93.79
Mode 2	Analytical	426.92	369.39	375.22
	Ansys	426.56	369.03	374.85
Mode 3	Analytical	960.59	832.12	844.25
	Ansys	956.60	829.11	842.18

SiC/Aluminium Composite presented the highest Natural frequency in all the modes that have been considered between Aluminium and Steel. This is due to the higher stiffness and lower density of SiC/Aluminium composite hence natural frequencies of the structure occur at higher values. Aluminium is given higher stiffness by reinforcing with SiC particles and this in turn improves the vibrational behavior of the composite. Natural frequencies for Aluminium are found to be less than those of SiC/Aluminium composite but close to that of Steel.

Aluminium has been found to have a lower density than Steel but the modulus of elasticity is lower; this results in Aluminium and Steel materials having similar natural frequencies. Natural frequencies of Steel are slightly higher than that of the Aluminium across all modes. However, a comparison between Aluminium and Steel shows that the two are not very different, and hence have very close values of the vibrational frequency.

(ii). ANSYS Graphical results for SiC/Aluminium beam

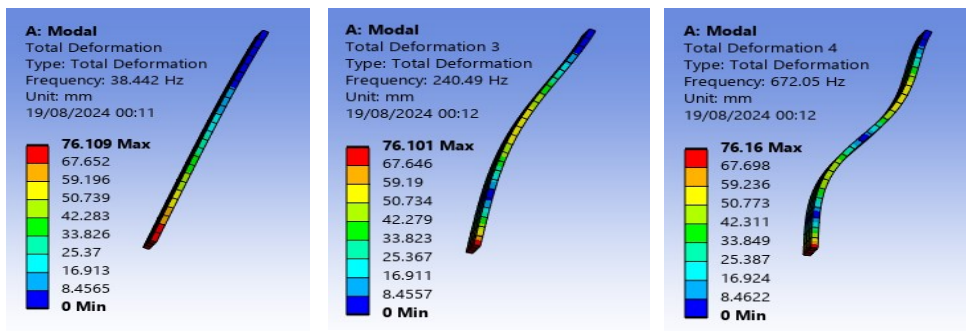


Figure 1 C-F first three Mode Shapes for SiC/Aluminium beam.

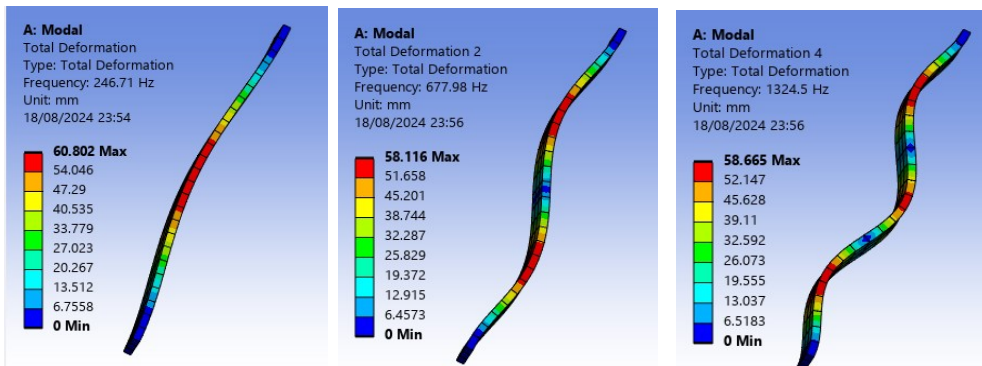


Figure 2 C-C first Mode Shapes for SiC/Aluminium beam.

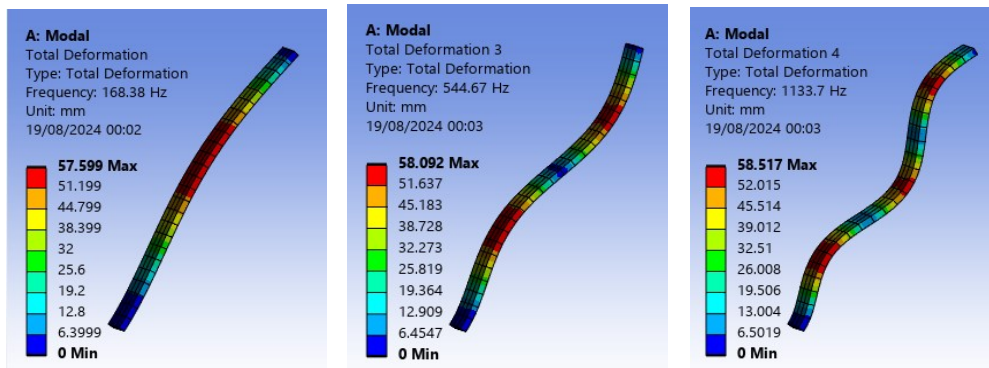


Figure 3 C-SS first Mode shapes for SiC/Aluminium beam.

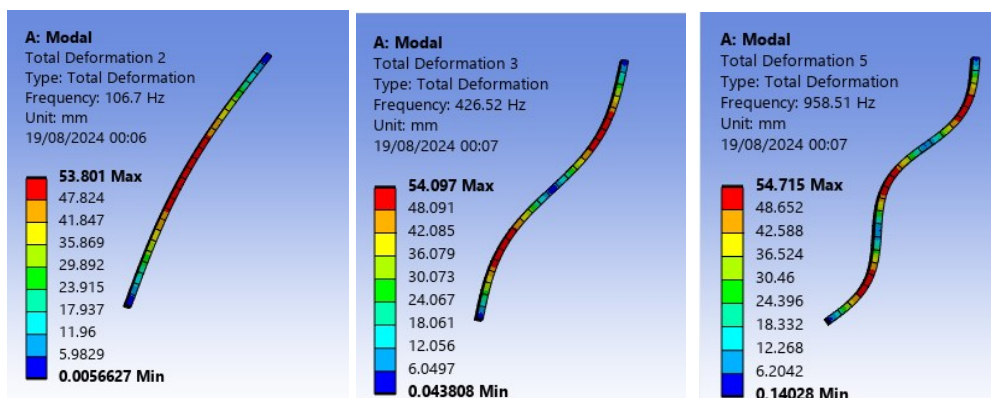


Figure 4 SS-SS first Mode shapes for SiC/Aluminium beam.

(iii). Comparative analysis between Analytical and ANSYS Results – Results for SiC/Aluminium Composites are considered for clamped-free beam as an example.

The differences in results obtained by the two methods are expressed in percentages. These percentages are obtained as follows. If the three modes of vibration $n = 1, 2, 3$, analytical natural frequency as $f_{n \text{ analytical}}$ and Ansys natural frequency as $f_{n \text{ ansys}}$, then:

$$\text{Percentage deviation} = \left(\frac{f_{n \text{ analytical}} - f_{n \text{ ansys}}}{f_{n \text{ analytical}}} \right) \times 100\%$$

The Analytical and Ansys natural frequencies differ by -1.12%, -0.93%, and -0.77% under C-F boundary conditions beam, -1.98%, -1.66%, and -1.31% under C-C boundary conditions, -1.00%, -0.81% and -1.31% under C-SS boundary conditions and 2.92%, 0.08% and 0.42% under SS-SS boundary conditions.

Figure 5 shows the close conformity of solutions obtained by analytical and the Ansys approaches for all the materials

and modes. These variations include the analytical approximations made during analysis and would fall below 1%. Comparing Mode 1 for the SS-SS beam, it is safe to say that the SiC/Aluminium composite diverged most (3.02 Hz or about 2.9% deviation) from the actual, probably due to some difficulties in accurately simulating the composite material. For modes 2 and 3, the difference in the analytical solution and the Ansys solution is lower for higher frequency modes indicating that the models are more accurate at higher modes. This could be because higher modes are less sensitive to the boundary condition.

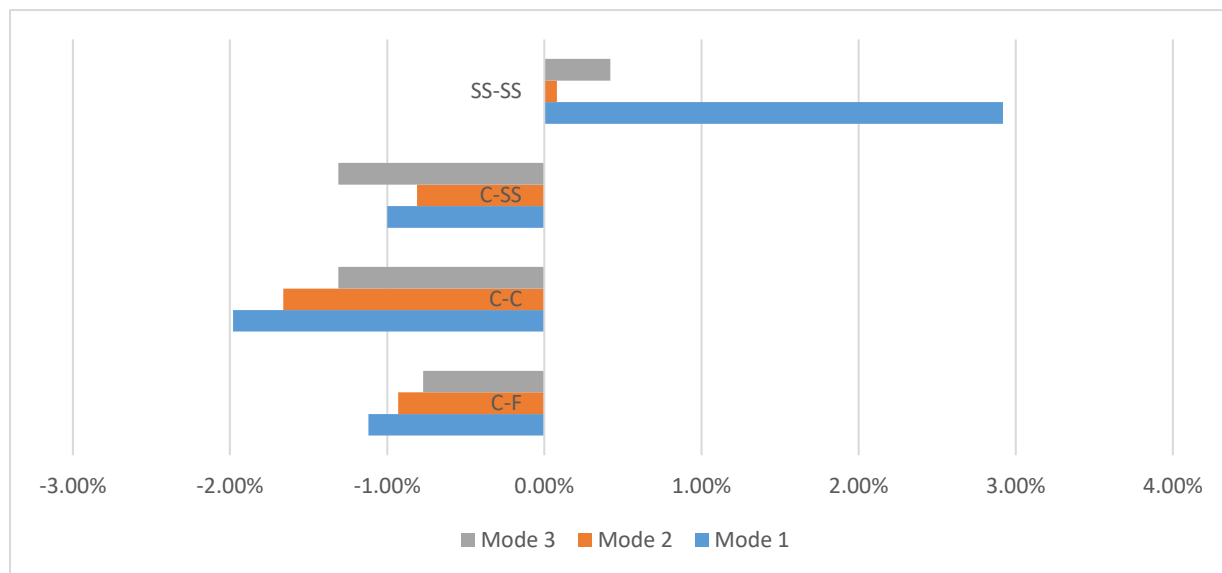


Figure 5 Percentage deviation in natural frequency obtained by Analytical and Ansys.

(iv). Effects of boundary conditions - Results for SiC/Aluminium Composites are considered as an example.

The results for SiC/Aluminium are extracted from Tables 2 to 5 and populated as shown in Table 6. For the C-F boundary condition natural frequencies are lowest compared to C-C, C-SS, and SS-SS across all modes. Thus,

the C-F condition provides more displacement at the free end resulting in low stiffness and consequently low natural frequencies.

Table 6 Natural frequencies of SiC/Aluminium beam supported by different boundary conditions.

Boundary Conditions	Analysis Method	Natural Frequency 'f' in Hz for SiC/Aluminium Composite Beam			
		C-F	C-C	C-SS	SS-SS
Mode 1	Analytical	38.02	241.95	166.74	109.92
	Ansys	38.445	246.73	168.4	106.71
Mode 2	Analytical	238.29	666.94	540.33	426.92
	Ansys	240.51	678.04	544.72	426.56
Mode 3	Analytical	666.98	1307.47	1127.36	960.59
	Ansys	672.11	1324.60	1133.80	956.60

The C-C boundary condition provided the highest natural frequency across all modes. This condition provides much no freedom of movement of the beam hence resulting in high stiffness and high natural frequencies. The C-SS boundary condition resulted in natural frequencies higher than C-F and SS-SS but lower than C-C conditions. The C-SS has one end restraint and the other end is free to rotate.

These conditions provide intermediate natural frequencies. The SS-SS boundary conditions result in natural frequencies lower than C-SS and higher than C-F. This condition also permits some extent of rotation at the supports which results in a lower degree of stiffness as compared to C-C. Figures 6, 7, and 8 provide graphical representations of the impact of boundary conditions on the natural frequencies of beams.

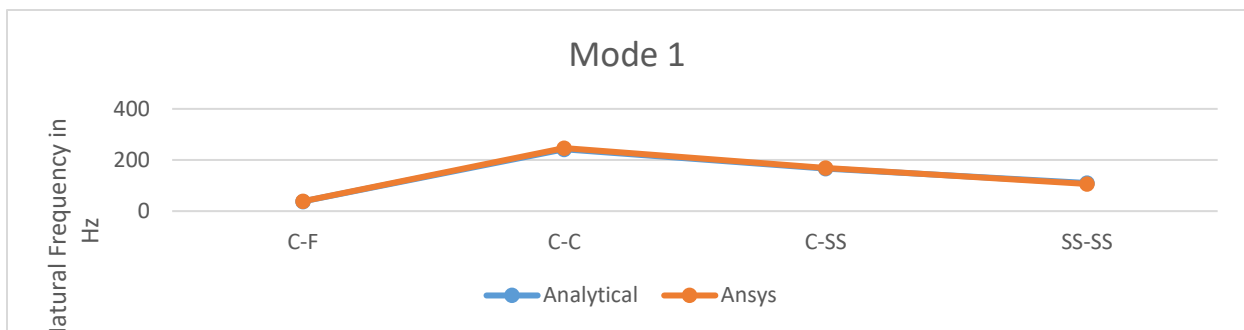


Figure 6 Mode 1 natural frequencies versus boundary conditions.

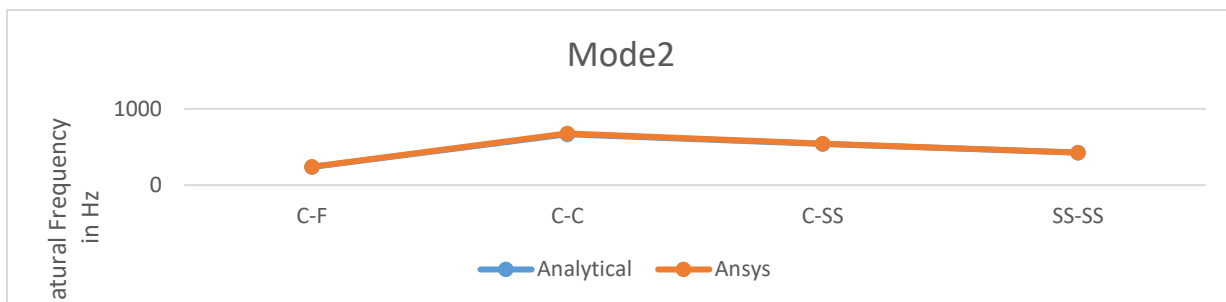


Figure 7 Mode 2 natural frequencies versus boundary conditions

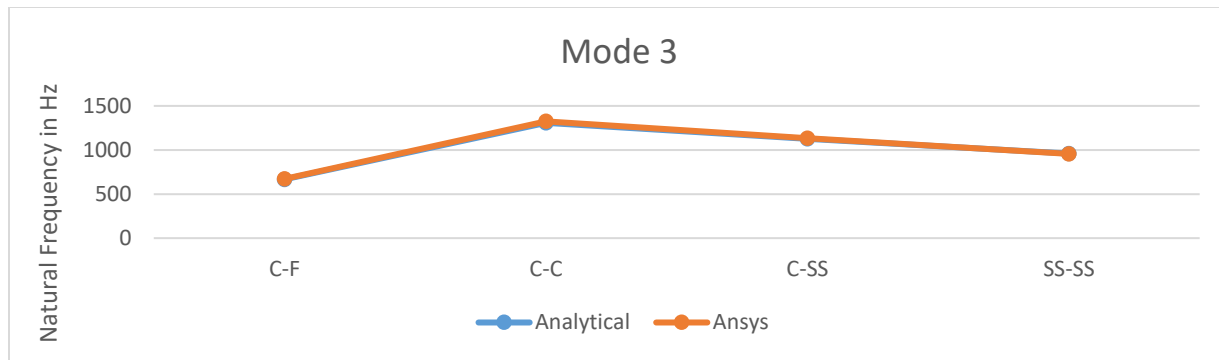


Figure 8 Mode 3 natural frequencies versus boundary conditions.

(v). Effects of specific modulus on natural frequencies of the beam.

The properties of the material determine the basic associated frequencies of vibration of beams. The beam material has a unique property called Specific Modulus (E/ρ) which has to be considered

Properties of Materials

SiC/Aluminium $E_c = 96.14 \text{ Gpa}$, $\rho = 2777\text{kg/m}^3$, $\frac{E}{\rho} = 34.62 \times 10^6 \text{m}^2/\text{s}^2$

Aluminium $E = 70 \text{ Gpa}$, $\rho = 2700\text{kg/m}^3$, $\frac{E}{\rho} = 25.93 \times 10^6 \text{m}^2/\text{s}^2$

Steel $E = 210 \text{ Gpa}$, $\rho = 7850\text{kg/m}^3$, $\frac{E}{\rho} = 26.75 \times 10^6 \text{m}^2/\text{s}^2$

Table 7 Natural frequencies versus boundary conditions at specific modulus of materials.

Boundary Condition	Mode	Specific Modulus		
		25.93	26.75	36.62
C-F	Mode 1	32.9	33.42	38.02
	Mode 2	206.17	209.43	238.29
	Mode 3	577.08	586.2	666.98
C-C	Mode 1	209.34	212.65	241.95
	Mode 2	577.05	586.17	666.94
	Mode 3	1131.25	1149.13	1307.47
C-SS	Mode 1	144.26	146.54	166.74
	Mode 2	467.51	474.89	540.33
	Mode 3	975.42	990.83	1127.36
SS-SS	Mode 1	92.35	93.81	109.92
	Mode 2	369.39	375.22	426.92
	Mode 3	832.12	844.25	960.59

Analytical results from Tables 2 to 5 are used to generate Table 7 above. The data in Table 7 are used to generate Figure 9 below. The specific modulus is one of those parameters which determine the natural frequency of a given material. Generally, a higher value of specific modulus results in higher natural frequencies, because the material is stiffer or the structure is lighter. SiC/Al (Specific Modulus = 36.62×10^6) used in the present study exhibits the highest natural frequencies across all the boundary conditions and modes. Consequently, the higher specific

modulus of the SiC/Al means higher stiffness resulting in higher resistance to deformation and thus, higher natural frequencies. Steel (Specific Modulus = 26.75×10^6) exhibits natural frequencies a little higher than Aluminium, but lower as compared to SiC/Al. Steel material has a higher density compared to aluminium and a relatively higher elastic modulus and therefore natural frequencies. Aluminium (Specific Modulus = 25.93×10^6) has the lowest specific modulus among the three materials resulting in the lowest natural frequencies. Due to it having a lower stiffness

the material can undergo larger deformation than the other two materials, which in turn lowers natural frequencies. From Figure 9, it was noted that the natural frequency increases with an increase in the Specific Modulus of the material. The rate of increase in natural frequency is more pronounced in the C-C mode 3 condition, followed by the C-SS mode 3 condition, and SS-SS mode 3 condition. The intermediate increase was noted at C-C mode 2 and C-F mode 3 conditions, followed by C-SS mode 2 condition, and SS-SS mode 2 condition. The low increase was noted at C-C mode 1 and C-F mode 2 condition, followed by C-SS

mode 1 condition, SS-SS mode 1 condition and C-F mode 1 condition. The frequency curve of the beam at C-F mode 1 condition can be noted to be a horizontal line. This signifies that the effect of material properties on the natural frequency of the C-F mode 1 is insignificant. This observation portrayed the effect of boundary conditions on the vibration of the beam. The boundary condition does offer a different stiffness effect to the beam; thus, the free end of the C-F beam lowers the stiffness, hence in result lowers the natural frequencies of vibration.

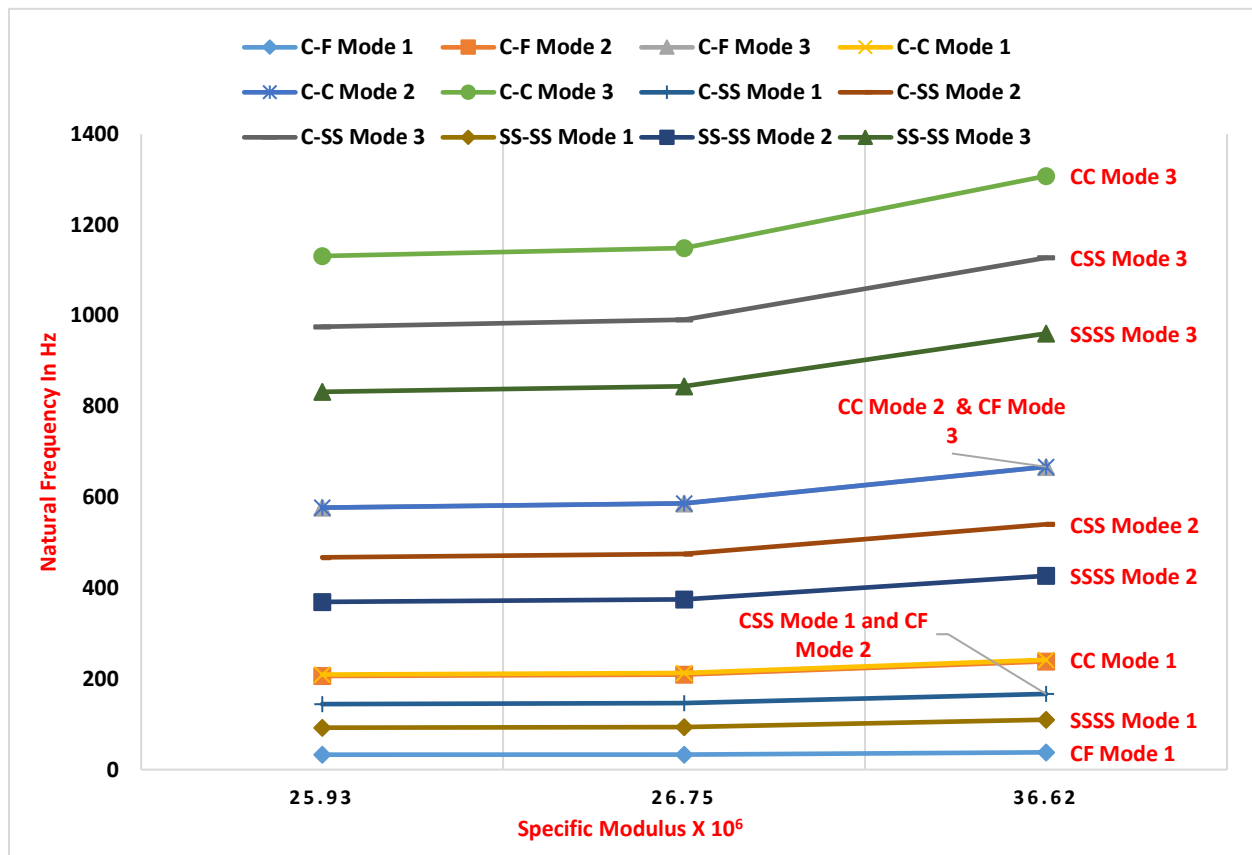


Figure 9 Natural frequencies versus Specific Modulus.

(vi). Effects of Cross-section area of the beam on the natural frequencies of vibration.

For the presentation of this study, a beam of the following characteristics was considered. The Length = 500mm, Cross-section area A1=0.0005m², A2= 0.0008m², A3= 0.0015m². The Physical properties of SiC/Aluminium composite are Density = 2777kg/m³, and Estimated Young Modulus of Elasticity = 96.14 GPa.

Table 8 Natural frequency for Beam under four different boundary conditions versus cross-area

Boundary conditions	Mode 'n' of Vibration	Natural Frequency in Hz		
		A1	A2	A3
C-F	Mode 1	38.02	76.04	114.06
	Mode 2	238.29	476.56	714.79
	Mode 3	666.98	1333.91	2000.74
C-C	Mode 1	241.95	483.88	725.78
	Mode 2	666.94	1333.84	2000.64
	Mode 3	1307.47	2614.86	3922.05
C-SS	Mode 1	166.74	333.46	500.16
	Mode 2	540.33	1080.63	1620.85
	Mode 3	1127.36	2254.65	3381.76
SS-SS	Mode 1	109.92	213.46	320.17
	Mode 2	426.92	853.83	1280.66
	Mode 3	960.59	1921.11	2881.49

From the consideration, the beam has a fixed length (L) and material properties, thus, Figure 10 depicts the natural frequency of vibrations to increase linearly with an increase in cross-section area. The rate of an increase in natural frequency is more pronounced for the C-C boundary condition, followed by C-SS, SS-SS, and C-F. These effects happen because the mode shape constant β for C-C and C-SS are higher compared to SS-SS and C-F boundary conditions. This underscores the role boundary conditions play as the C-C condition yields the highest frequencies due to maximum stiffness and the C-F condition yields the lowest due to greater flexibility.

(D). CONCLUSIONS

The natural frequencies for the beam under four different boundary conditions were estimated analytically and numerically using ANSYS Workbench. The results obtained were consistently in agreement for both methods. It was noted that higher natural frequencies were achieved by SiC/ Aluminium composite beams across all four boundary conditions considered, followed by structural Steel and Aluminium beams. This is because SiC/ Aluminium composites have a higher specific modulus than Steel and Aluminium.

The higher natural frequency is experienced in C-C boundary conditions, followed by C-SS, SS-SS, and lower in C-F boundary conditions. The linear increase in natural frequencies is depicted to increase with the beam cross-sectional area when the horizontal length and mass distribution of the beam are constant. The rate of increase in the natural frequency is more pronounced in C-C boundary conditions, followed by C-SS, SS-SS, and least under C-F boundary conditions.

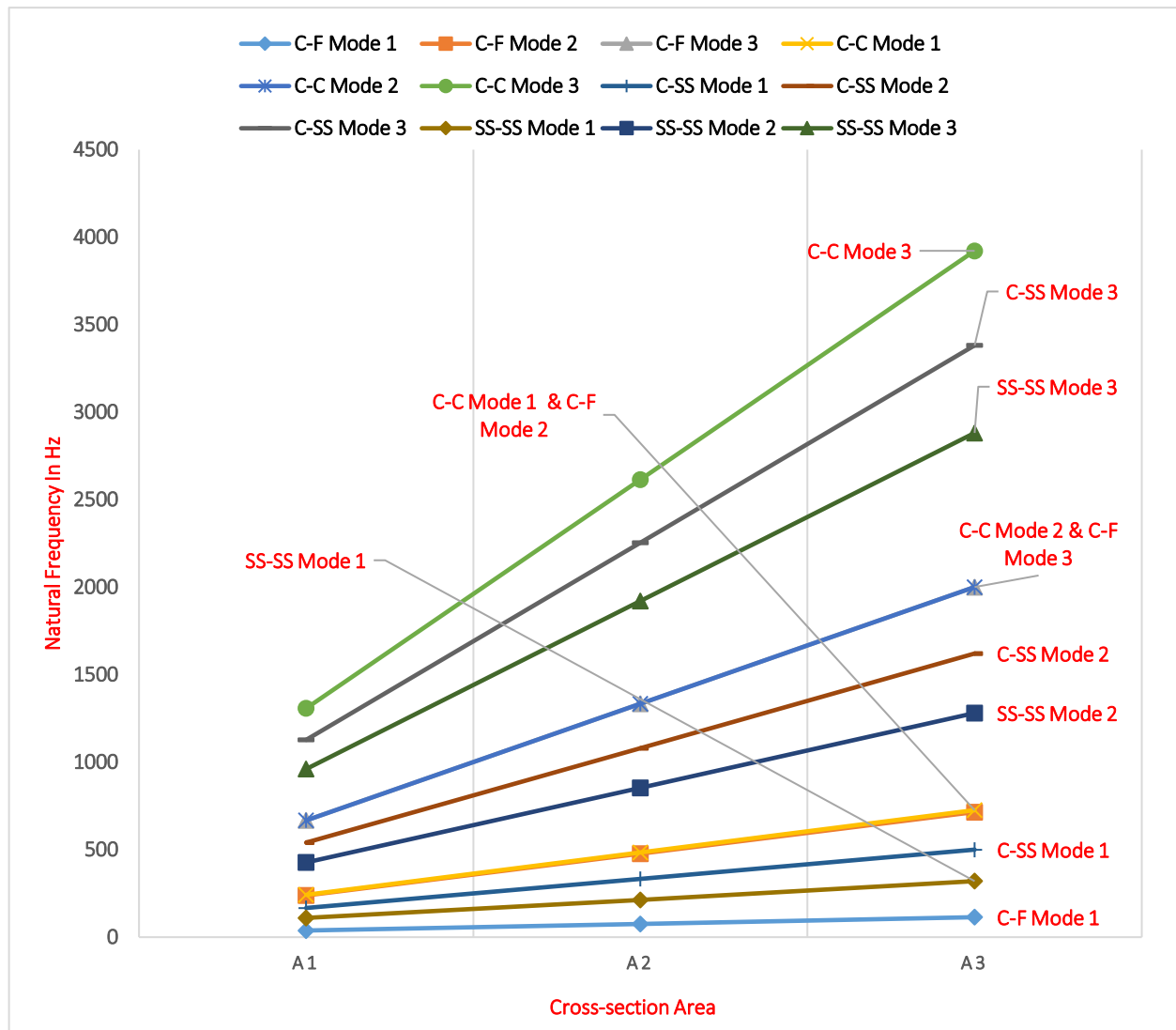


Figure 10 Natural frequency versus cross-section area at different boundary conditions.

REFERENCES.

[1] Lu J., Qiu T., Chen Z., Zhang W., Wu M., and Du C. (2023). Study of vibration frequency-fatigue strength action of 6061-T6 aluminium alloy during fillet welding. *Journal of Vibroengineering*.

[2] Mufazzal1, S., Muzakkir, S.M., and Zakir H.J. (2017). Investigation of the Effect of Material on Undamped Free Vibration of Cantilever Beams with Uniform Single Surface Crack. *Proceedings of IOP Conf. Series: Journal of Materials Science and Engineering*. 225.

[3] Agarwallaa, D.K, and Parhib, D.R., (2013). Effect of Crack on Modal Parameters of a Cantilever Beam Subjected to Vibration. *Proceedings of the Chemical, Civil and Mechanical Engineering Tracks of the 3rd Nirma University International Conference (NUIICONE 2012)*, *Procedia Engineering*, 51, 665 – 669.

[4] Nikhil, Y., and Jeyashree, T. M. (2016). Dynamic Response of a Cracked Beam under Free Vibration. *International Journal of Civil, Structural, Environmental and Infrastructure Engineering Research and Development (IJCSIEIRD)*, 6(2), 45-56.

[5] Mia, M.S., Islamb, M.S., and Ghos, U. (2017). Modal Analysis of Cracked Cantilever Beam by Finite Element Simulation. *Proceedings of 10th International Conference on Marine Technology, MARTEC 2016, Procedia Engineering*. 194, 509 – 516.

[6] Gawande, S. H., and More, R. R. (2016). Some Investigations on Effect of Notch on Dynamics Characteristics of Cantilever Beams. *International Journal of Acoustics and Vibration*, 24(1), 20-27.

[7] Kuppast, V.V., Chalwa, V.K.N., Kurbet, S.N. & Yadawad, A.M. (2014) Finite Element Analysis of Aluminium Alloys for their Vibration Characteristics. *International Journal of Research in Engineering and Technology*, 3(3), 2321-7308

[8] Abdellah, M.Y, Alharthi, H., Husein, E., Abdal-hay, A. and Abdel-Jaber, G.T. (2021). Finite Element Analysis of Vibration modes in Notched Aluminum Plate. *Journal of Mechanical Engineering Research and Developments*. 44(10), 343-353

- [9] Derkach, O., Zinkovskii, A., Onyshchenko, Y., and Savchenko, V. (2022). Notch-type damage influence on the frequency of the principal mode of the composite cantilever beam flexural vibrations. *Procedia Structural Integrity*, 36, 71–78.
- [10] Quila, M., Ch. Mondal, P. S., and Sarkar, P. S. (2014). Free Vibration Analysis of an Un-cracked & Cracked Fixed Beam. *IOSR Journal of Mechanical and Civil Engineering*, 11(3), 76–83.
- [11] Ferreira, G.V., & Neto, F.L. (2016). Modal Analysis of Hybrid Adaptive Beams. *Proceedings of the XXXVII Iberian Latin-American Congress on Computational Methods in Engineering*, 6-9.
- [12] Avcar, M. (2014). Free Vibration Analysis of Beams Considering Different Geometric Characteristics and Boundary Conditions. *International Journal of Mechanics and Applications*, 4(3), 94–100.
- [13] Haskul, M., and Kisa, M. (2021). Free vibration of the double tapered cracked beam. *Inverse Problems in Science and Engineering*, 29(11), 1537–1564.
- [14] Rossit, C., Bambill, D., Ratazzi, A., and Maiz, S. (2015). Vibrations of L-Shaped Beam Structures with a Crack: Analytical Approach and Experimental Validation. *Experimental Techniques*.
- [15] Wang, J., and Qiao, P. (2007). Vibration of beams with arbitrary discontinuities and boundary conditions. *Journal of Sound and Vibration*, 308(1–2), 12–27.
- [16] Charoensuk, K., and Sethaput, T. (2023). The Vibration Analysis Based on Experimental and Finite Element Modeling for Investigating the Effect of a Multi-Notch Location of a Steel Plate. *Applied Sciences*, 13(21), 12073.
- [17] Shah, S.S., Sharma, M, and Sharma, P. (2019). Vibration Analysis of Composite Beam. *International Journal for Technological Research in Engineering*, Volume 6 (issue 12), 2347–4718.
- [18] Bozkurt, S., Tarik, M., and Ozturk, B. (2011). Transverse Vibration Analysis of Euler-Bernoulli Beams Using Analytical Approximate Techniques. *Advances in Vibration Analysis Research*.
- [19] Nalbant, M. O., Bagdatli, S. M., and Tekin, A. (2023). Free Vibrations Analysis of Stepped Nanobeams Using Nonlocal Elasticity Theory. *Scientia Iranica*,
- [20] Teggi, H. (2020). Free Vibration Analysis of Composite Beam Considering Different Boundary Conditions using Finite Element Method. *International Journal for Research in Applied Science and Engineering Technology*, 8(8), 1410–1422.
- [21] Santhosh, N., Ramesha K, Chennakeshava, R., and Manjunath N (2019). Vibration Characterization of Reinforced Aluminium Composite Plates. *Journal of Engineering Science and Technology*
- [22] Bozkurt, Y., and Ersoy, S. (2016). Determining the vibration behavior of metal matrix composite used in aerospace industry by FEM. *Vibroengineering Procedia*, 9, 29–32.
- [23] Acharya, S.S.R., Suresh, P.M., and Suresh, R. (2021). Vibration Characteristics of Aluminium Reinforced with SiC – A Review, *International Journal of Engineering Research & Technology (IJERT)*.
- [24] Kumar, P. S. S. R., Smart, R., Alexis, S., and Ramanathan, S. (2017). Modal analysis of mwcnt reinforced aa5083 composite material. *ResearchGate*.
- [25] Taj, N. A., Doddamani, N. S. S., and Vijaykumar, N. T. N. (2017). Vibrational Analysis of Aluminium Graphite Metal Matrix Composite. *International Journal of Engineering Research and Technology*, V6(04).
- [26] Lakshmikanthan, A., Mahesh, V., Prabhu, R., Patel, M., and Bontha, S. (2020). Free Vibration Analysis of A357 Alloy Reinforced with Dual Particle Size Silicon Carbide Metal Matrix Composite Plates Using Finite Element Method. *Archives of Foundry Engineering*, 101–112.